A Combined Coding and Modulation Approach for Communication over Dispersive Channels

DAVID CHASE

Abstract—The concept of combining the design of the error-correcting-coding approach and the modulation format is treated in general terms and its effectiveness is demonstrated by a specific implementation referred to as Codem I. A new decoding algorithm is presented, which has the interesting property that the only channel measurement information utilized is the relative reliability of each received digit. The effectiveness of this decoding technique is demonstrated by computer simulation over three different channel models for dispersive channels. Comparisons of the performance of Codem I with the more conventional 16-tone (four-phase DPSK) HF modem are obtained by actual field results as well as by computer simulations. Improvement in error probability in the region of two orders of magnitude is demonstrated when both systems are operating under similar channel conditions and at equal data rates. A further improvement is demonstrated when channel measurement information is used to reject a small percentage (typically less than 3 percent) of codewords that are considered unreliable.

I. Introduction

IN THIS PAPER, a modulation and error-correcting-coding approach will be described, which is particularly effective for communicating over dispersive channels such as the HF channel. This technique is unconventional in that the coding and modulation format are jointly designed to enhance the effectiveness of the overall communication system. The demodulation of the received signal is accomplished in such a manner that meaningful channel measurement information can be supplied to the error-correcting decoder. A new decoding algorithm is presented, which utilizes this information to significantly improve the performance over conventional binary decoding techniques.

Some of the concepts presented in this paper have resulted in the development of an experimental modem for HF communications, referred to as Codem I, which will be used to make the ideas presented more concrete. Nevertheless, it is not the intent of this paper to completely describe Codem I, since this equipment has features that would be inappropriate to be covered in this paper. On the other hand, the results presented here should not be construed to be applicable only to HF communications. Indeed, there is some indication that these concepts are quite applicable for transmission over telephone lines and that the generalized decoding algorithm presented has applications even for nondispersive channels.

The problem of obtaining reliable transmission of digital information over channels characterized by multipath and fading phenomena has always presented a significant challenge for the communicator. Even for an effective modulation scheme, the time-varying nature of these channels produces an irreducible error rate [1] that cannot be overcome by increasing the transmission power. Error-correcting-coding techniques have been applied to channels of this nature [2] and have yielded a significant improvement in error probability, but at the expense of a loss in data rate, which is typically on the order of 50 percent, i.e., a rate $\frac{1}{2}$ code is employed. Another characteristic of the conventional application of error-correcting coding is overall delay introduced in a system, which is required to combat the clustering of error occurrences on the HF channel. This delay, typically on the order of a few seconds, may or may not be tolerable depending on the particular communication application. The Codem approach enables one to apply coding and still maintain the overall data rate by modifying the modulation approach to accommodate the code. Furthermore, the use of channel measurement in the decoding process enables one to obtain a significant performance improvement without introducing an overall system delay beyond one data frame.

In Section II of this paper the modulation approach, the extraction of channel measurement information, and the decoding algorithm for the use of this information are described. The decoding algorithm presented applies only to a special class of codes but has the interesting property that only the relative amplitude, or rank, of the available channel measurement information is used in the decoding process.

Evaluating communication techniques for dispersive channels requires a careful specification of the particular channel model assumed and, even then, the results obtained are only as realistic as the assumed model. Three different channel models are discussed in detail in Section III and computer-simulated results comparing Codem I to the more conventional 16-tone four-phase DPSK modem are presented in Section IV. Actual field-test results comparing these two systems are also covered in Section IV. These results are interesting in that the actual HF link tests bring out some of the virtues as well as some of the inadequacies of computer simulations.

In the final section of this paper, the results obtained are discussed and some extensions of the Codem principles are mentioned.

Paper approved by the Communication Theory Committee of the IEEE Communications Society for publication without oral presentation. Manuscript received August 17, 1972; revised October 30, 1972. This work was supported in part by the Department of the Navy under Contracts N00019-68-C-0376 and N62269-70-C-0061.

The author was with the General Atronics Corporation, a subsidiary of the Magnavox Company, Philadelphia, Pa. 19118. He is now with CNR, Inc., Newton Upper Falls, Mass. 02164.

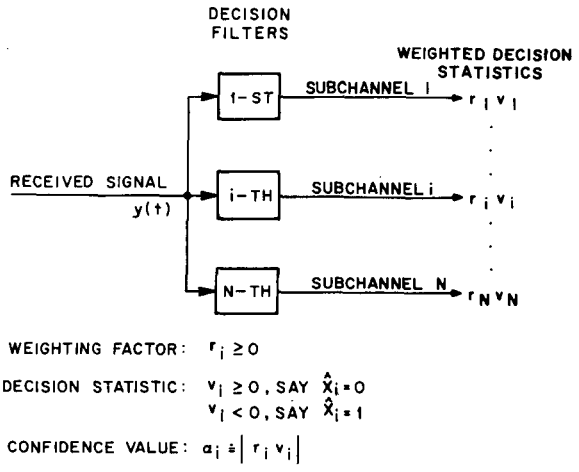

Fig. 1. General waveform receiver.

II. The Codem Concept

This section will be divided into two parts. The first will deal with the modulation approach used for signaling over a dispersive channel and the extraction of the required channel measurement information from the received waveform. The second part of this section deals with the channel measurement decoding algorithm and stands somewhat independently of the particular modulation approach.

A. Modulation Approach

In the general case the transmitted waveform $x(t)$ is specified by a set of binary digits given by $X = X_1, X_2, \cdots, X_N$. The received signal given by $y(t)$ is first processed by a waveform receiver as shown in Fig. 1. The decision statistic for each binary digit, given by v_i, is assumed to be of the form that a positive value indicates a 0 and a negative value indicates that a 1 was transmitted. Each decision statistic is weighted by a positive number denoted by r_i, which can be viewed as the gain for the ith subchannel. The magnitude of the weighted decision statistic will be used by the decoder as a measure of the reliability or confidence value of each received bit. In a conventional communication system, when diversity combining is employed, the outputs of several of these decision filters are summed together to obtain a single estimate of a transmitted bit [3]. The exact form of these decision filters depends on the modulation format and the channel as will be illustrated for the Codem signaling format.

The specific modulation approach used in Codem I is differential phase shift keying (DPSK) of a set of $N = 25$ orthogonal (parallel) tones with one of four phases. Thus, the normalized transmitted signal is given by

$$x(t) = \sum_{i=1}^{N} \sqrt{2} \cos(\omega_i t + \theta_i), \tag{2-1}$$

where θ_i is the phase angle of the ith tone and ω_i is 2π times a multiple of the reciprocal of the integration time denoted by T.

For a four-phase DPSK signal scheme θ_i is assumed to be determined by a pair of bits X_{ci} and X_{si} according to the following relationship:

$$\theta_i = \begin{cases} \theta_i' + \pi/4, & X_{ci}, X_{si} = 0, 0 \\ \theta_i' + 3\pi/4, & X_{ci}, X_{si} = 1, 0 \\ \theta_i' - 3\pi/4, & X_{ci}, X_{si} = 1, 1 \\ \theta_i' - \pi/4, & X_{ci}, X_{si} = 0, 1 \end{cases} \tag{2-2}$$

where θ_i' is the phase angle of the ith tone in the previous frame.

A waveform of this nature is attractive for a multipath channel since the received waveform will still be a set of sine waveforms after the duration of the impulse response. Thus, if the impulse response of the channel is represented by a function $h(t)$ and is of duration $\Delta\tau$ we have

$$y(t) = \int x(\tau) h(t - \tau)\, d\tau = \sum_{i=1}^{N} \sqrt{2} r_i \cos(\omega_i t + \theta_i + \gamma_i) + n(t), \quad t \geq \Delta\tau \tag{2-3}$$

where r_i and γ_i are unknown variables determined by the impulse response of the channel and $n(t)$ is assumed to be a white Gaussian process with a one-sided noise power spectrum given by N_0 and thus an impulse autocorrelation function given by $R(\tau) = (N_0/2)\delta(\tau)$. In general, the impulse response of the channel is time varying and thus r_i and γ_i may also vary with time.

If the time between phase keying the signal T_f is chosen larger than the integration time T, the effects of the multipath can be minimized by having a guard time T_g at the start of each frame interval before integration. Thus, by choosing $T_f - T = T_g > \Delta\tau$, the major effect of the multipath is the introduction of the random amplitude r_i and random phase γ_i on each tone. Depending on the channel model (see Section III), these random amplitudes can readily vary by as much as a factor of 10 (20 dB) across the set of phased-keyed tones. This selective fading effect can severely limit the performance of a parallel tone modem but can be overcome by decoding with channel measurement information.

In order to abstract the required channel measurement information the weighted decision statistic for each transmitted bit must be calculated. By correlating the received signal with a quadrature set of reference tones, the cosine and sine components obtained are given by

$$u_i = \frac{1}{T} \int_{T_g}^{T_f} y(t) \sqrt{2} \cos \omega_i t dt = r_i \cos(\theta_i + \gamma_i) + n_{ci} \tag{2-4a}$$

$$v_i = \frac{1}{T} \int_{T_g}^{T_f} -y(t) \sqrt{2} \sin \omega_i t dt = r_i \sin(\theta_i + \gamma_i) + n_{si}. \tag{2-4b}$$

Time synchronization is assumed so that multipath effects can be gated out. The components n_{ci} and n_{si} resulting from the white noise Gaussian process $n(t)$ are statistically independent, have zero mean, and a variance of $\sigma^2 = N_0/2T$.

In order to obtain our bit estimate, the receiver uses the phase of the previous frame as a reference for the present frame. If u_i' and v_i' are the sine and cosine components for

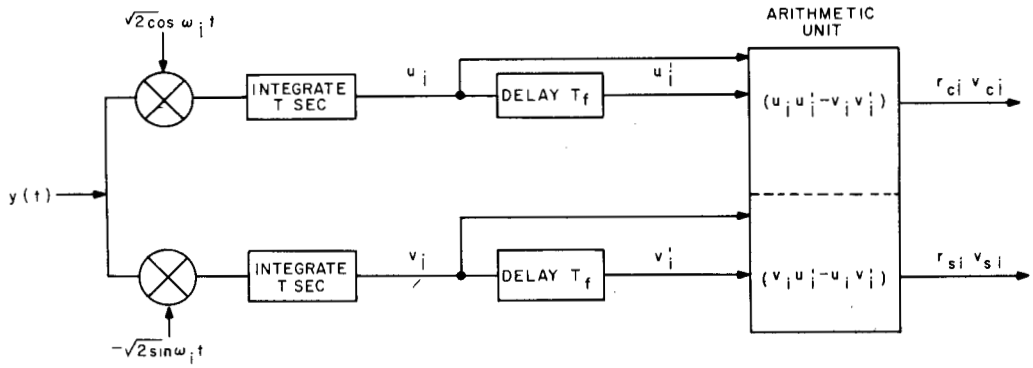

Fig. 2. Pair of decision filters for a four-phase DPSK modulation scheme.

the previous frame, the phase change is given by

$$\Delta\theta = \tan^{-1}\left(\frac{u_i}{v_i}\right) - \tan^{-1}\left(\frac{u_i'}{v_i'}\right) \tag{2-5}$$

and the decision rule becomes

$$\begin{aligned} \hat{X}_{ci} &= 0, \quad \cos\Delta\theta \geqslant 0 \\ \hat{X}_{ci} &= 1, \quad \cos\Delta\theta < 0 \\ \hat{X}_{si} &= 0, \quad \sin\Delta\theta \geqslant 0 \\ \hat{X}_{si} &= 1, \quad \sin\Delta\theta < 0. \end{aligned} \tag{2-6}$$

This decision rule is valid regardless of the arbitrary phase angle of the quadrature set of reference tones, which was assumed to be zero in (2-6). Equation (2-6) is equivalent to determining in which of the four quadrants $\Delta\theta$ falls. Note that for the particular four-phase Gray code, we can determine X_{ci} by the sign of $\cos\Delta\theta$ and determine X_{si} by the sign of $\sin\Delta\theta$.

This decision rule can be simplified by obtaining an equivalent rule that does not require the calculation of $\Delta\theta$ and, furthermore, gives us the desired weighted decision statistic. To obtain this rule we write the sine and cosine components of the present and past frame in terms of the phasors given by

$$z_i = u_i + jv_i \tag{2-7}$$

and

$$z_i' = u_i' + jv_i'. \tag{2-8}$$

The real part of the product of the present phasor and complex conjugate of the past phasor yields

$$\text{Re}\,[z_i \cdot z_i'^*] = |z_i||z_i'|\cos\Delta\theta = u_i u_i' - v_i v_i' \tag{2-9}$$

and the imaginary part yields

$$\text{Im}\,[z_i \cdot z_i'^*] = |z_i||z_i'|\sin\Delta\theta = v_i u_i' - u_i v_i'. \tag{2-10}$$

Since $|z_i|$ and $|z_i'|$ are positive, the decision rules given by (2-6) are equivalent to using the sign of (2-9) to determine $\hat{X}_{ci}$ and the sign of (2-10) to determine the value of $\hat{X}_{si}$. The statistics given by (2-9) and (2-10) will be denoted by $r_{ci}\,v_{ci}$ and $r_{si}\,v_{si}$, respectively, and their magnitudes will be used as our confidence values. The pair of decision filters required to abstract the channel measurement information from the ith tone are illustrated in Fig. 2.

Some justification of the form of the decision filters given in Fig. 2 is obtained by noting that under the appropriate approximations the conditional probability of decoding X_{ci} correctly, for a given z_i and z_i', increases monotonically with $|r_{ci}\,v_{ci}|$.

For the case when the decision statistic is positive, i.e., $\cos\Delta\theta > 0$, this conditional probability is given by

$$\begin{aligned} &\Pr\,[\text{correct decoding}|z_i, z_i'] = \Pr\,[X_{ci} = 0|z_i, z_i'] \\ &= \frac{p\,[|z_i|\cos\Delta\theta\,|X_{ci} = 0, z_i']}{p(|z_i|\cos\Delta\theta\,|X_{ci} = 0, z_i') + p(|z_i|\cos\Delta\theta\,\big|X_{ci} = 1, z_i')}. \end{aligned} \tag{2-11}$$

Note that when z_i' is given, the decision statistic for X_{ci} is just the projection of z_i onto z_i' or $|z_i|\cos\Delta\theta$. Also, to obtain the above expression we assume that $\Pr\,[X_{ci} = 0] = \Pr\,[X_{ci} = 1] = \frac{1}{2}$.

The previous conditional probabilities are Gaussian distributed with an actual mean value given by the projection of the complex value of r_i on z_i'. In our calculations this mean value will be approximated by

$$\mu = +|z_i'|/\sqrt{2}, \quad X_{ci} = 0$$

and

$$\mu = -|z_i'|/\sqrt{2}, \quad X_{ci} = 1.$$

Note that the noise-free value of the cosine of this angle is $\pm 1/\sqrt{2}$, and the estimated value of the fading variable r_i is obtained from the previous frame as $|z_i'|$. The variance in each of the conditional probabilities in (2-11) is $\sigma^2 = N_0/2T$, which is due to the Gaussian noise projection on the reference axis given by z_i'. Substituting these values into (2-11) yields

$$\Pr\,[X_{ci} = 0|z_i, z_i'] \simeq \frac{1}{1 + \exp\left[-\dfrac{4T}{\sqrt{2}N_0}|z_i||z_i'|\cos\Delta\theta\right]}, \tag{2-12}$$

which increases monotonically with $\alpha_{ci} \doteq |z_i||z_i'|\cos\Delta\theta$.

Similarly, for the case when the decision statistic is negative,

i.e., $\cos \Delta\theta < 0$, we can show that

$$\Pr[X_{ci} = 1 | z_i, z_i'] \simeq \frac{1}{1 + \exp\left[+\frac{4T}{\sqrt{2}N_0} |z_i||z_i'| \cos \Delta\theta\right]} = \frac{1}{1 + \exp\left[-\frac{4T}{\sqrt{2}N_0} \alpha_{ci}\right]} \quad (2\text{-}13)$$

and thus the same results hold. Note, that the confidence value α_{ci} is not only a function of the estimated received power in the ith channel, given by $|z_i||z_i'|$, but is also a function of the relative phase angle between z_i and z_i' as one would intuitively expect. Also, note that a confidence value of 0 corresponds to a conditional probability of $\frac{1}{2}$ for correct decoding, while a confidence value of ∞ corresponds to a conditional probability of 1 for correct decoding.

The same approximations can be used to show that a confidence value of α_{si} given by $|z_i||z_i'||\sin \Delta\theta|$ is also monotonically increasing with the probability of a correctly decoded X_{si} and thus the decision filters shown on Fig. 2 yield the desired weighted decision statistic. It should be noted that for the coherent fading channel, i.e., r_i and its phase are known *a priori*, no approximations are necessary to obtain the above results.

B. Coding Approach

The frequency selective fading resulting from the multipath spread causes some tones to have considerably less power than others and thus the error rate is essentially determined by the few tones of lowest amplitude (see the frequency spectrum shown in Section III). Using an error-correcting code across the frequency band can significantly reduce the effects of selective fading. The coding transformation introduces a dependency between the data bits, which enhances the reliability of those bits transmitted on tones of weak amplitude. The use of channel measurement information in conjunction with the error-correcting code greatly increases the effectiveness of the decoding process. Also, note that the code block synchronization problem is simplified when coding across the frequency band since once the modem obtains frame synchronization, block synchronization is also automatically obtained.

In the general case, for each frame a codeword composed of N binary digits, obtained from $K < N$ information digits, is fed into a digital data modulator. The waveform corresponding to these N digits $x(t)$ is transmitted over a channel and the received waveform $y(t)$ is processed by a waveform receiver. The output of the waveform receiver can be viewed as two N-dimensional vectors. The vector $Y = Y_1, Y_2, \cdots, Y_N$ is a binary vector containing the preliminary estimates of the codeword letters obtained from the sign of the weighted decision statistic. The vector $\alpha = \alpha_1, \alpha_2, \cdots, \alpha_N$ contains a set of real positive numbers that represents the confidence values for each received digit. The channel measurement decoder uses both the properties of the code and the confidence value to estimate the particular block of transmitted information digits. A block diagram of a communication system of this nature is illustrated in Fig. 3.

A particular channel measurement decoding algorithm will now be presented, which has the interesting property that only the rank, or relative amplitude of each α_i contained in α, will be used in the decoding process. Thus, each received digit is assigned a number between 1 and N depending on the relative amplitude of its confidence value. The number N is assigned to the most reliable digit, i.e., the digit with the largest confidence value. This algorithm will be applied to a code that is assumed to have a set of J orthogonal parity check equations [4], [5].[1]

The first step of this algorithm is to flag the $(d - 1)$ digits or bits of lowest rank, where d is the minimum distance of the code. This initial step is used to label a set of bits that has the lowest reliability. The next step is to start with the highest ranked bit and work downward as follows.

Step 1a: If all equations $\surd$, decode bit in question as is. (The bit is assumed correct if all its parity equations check.)

Step 1b: If all equations $\not\surd$, flag the given bit. (A flag indicates that the bit in question is considered unreliable.)

Step 1c: If at least one equation $\surd$, decode bit as is provided its rank is larger than the lowest ranked undecoded bit in each $\not\surd$ equation and flag the lowest ranked undecoded bit in each $\not\surd$ equation. (In this step we decode the bit in question only if there is an undecoded bit of lower rank in each parity equation that fails to check. The lowest rank undecoded bit is considered unreliable and thus is flagged.)

Step 2: If after decoding a given bit, there remains one undecoded bit in any equation in the present set of orthogonal equations, decode this bit, whether or not it is flagged, by forcing parity to check. (Only during this step is it possible to correct errors since a bit can now be inverted to force the given parity equation to check.)

Step 3: If all remaining bits are flagged, decode the highest ranked bit and proceed to Step 2. (This last step is necessary to guarantee that all received bits are eventually decoded.)

In order to further illustrate this decoding procedure an example will be given for a simple code (9, 4) of minimum distance 4. This code, illustrated at the top of Fig. 4, has a parity check on each row and column of the information digits that are arranged in a 2×2 matrix. The last parity digit P_9 is a parity check on the entire set of information digits. The row and column parity equations on each digit form the two orthogonal equations that will be used in the decoding algorithm. As an example, two orthogonal equations on I_3 are $I_3 \oplus I_4 \oplus P_6 = 0$ and $I_3 \oplus I_1 \oplus P_7 = 0$. A third orthogonal equation on I_3 given by $I_3 \oplus I_2 \oplus P_5 \oplus P_8 \oplus P_9 = 0$ will not be used in the following illustration.

At the start of the decoding procedure, Fig. 4I, the received digits with the $d - 1 = 3$ lowest confidence values are flagged

[1] A code is said to have J orthogonal equations if, for any given digit, there exist J parity check equations that involve this digit and no other digit appears in more than one of these J equations.

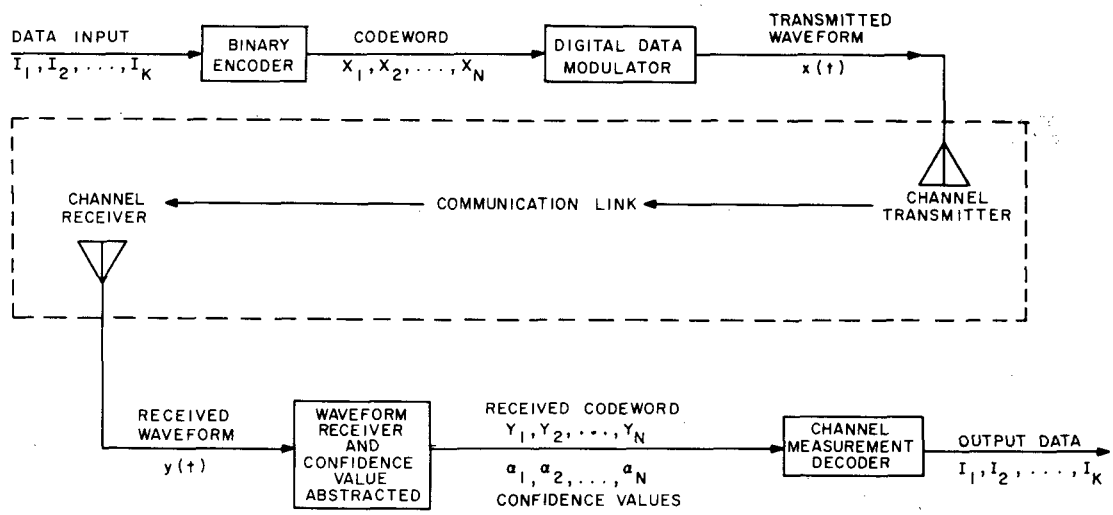

Fig. 3. Communication system employing block coding and channel measurement decoding.

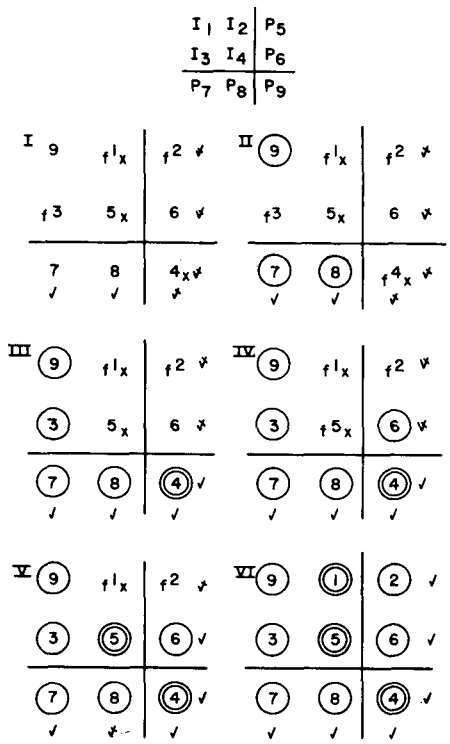

Fig. 4. Decoding a (9, 4) product code.

as indicated by the letter f on the left of the bits with rank numbers 1, 2, and 3. The x are used to indicate that the received sequence $Y_1, Y_2, \cdots, Y_9$ contains three errors on those bits of rank 1, 4, and 5. In Fig. 4II a circle is used to indicate that the bits of rank 9, 8, and 7 are decoded by Step 1a. An additional flag is also placed on the bit of rank 4 since it is the lowest rank bit in the $\surd$ equation for the bits of rank 8 and 7. Step 2 is used to decode the bits of rank 4 and 3 as indicated by Fig. 4III. The double circle is used to indicate that the bit with the rank of 4 is inverted and thus corrected. The bit of rank 6 is decoded next and the bit of rank 5 is flagged by Step 1c. At this point Step 2 is used to decode the remaining undecoded bits. In this particular illustration, parity is forced alternately in the row first, then the column of the newest decoded bit, i.e., the row of bit of rank 6, then the column of the bit of rank 5, then the row of the bit of rank 1. The same results would also have been obtained if parity were first forced in the column of the bit of rank 6, rather than its row.

In this particular example, three errors were corrected with the aid of channel measurement. A binary decoder could have only corrected one error for this distance 4 code. The effectiveness of this decoding algorithm will be further illustrated in Section IV. It should be noted [6] that for certain channels it can be shown that decoding with channel measurement information increases the error-correcting capability of a given code from $e = [(d - 1)/2]$ for a binary decoder to $(d - 1)$.

While the actual justification of this decoding algorithm will be given by computer and field test results, an interesting sufficient condition for decoding correctly will now be given.

Assume that the given code block contains error only in the $d - 1$ bits of lowest rank. Since the $d - 1$ bits of lowest rank are flagged, all the bits in error are flagged. Furthermore, since the code is of minimum distance d, the error pattern is detectable by the presence of several "$\surd$" parity equations. Parity on these $\surd$ equations will eventually be forced to check by Step 2 of this decoding algorithm. During this step all the errors must be corrected since under this condition all bits of rank greater than $d - 1$ are not inverted and thus are decoded correctly. Note that the bits of rank greater than $d - 1$ are decoded without change by Step 1 and Step 3 and cannot be inverted by Step 2 since all $\surd$ equations involve at least one flagged bit of rank $\leqslant (d - 1)$. Thus, we are guaranteed to correct all error patterns composed of bits with ranks less than d.

The probability that this sufficient condition is false, which is a necessary condition for a block error, yields an upper bound on the probability of decoding incorrectly. This proba-

bility can be written as

$$P_e[\text{block}] < \Pr[\exists \cdot Y_i \neq X_i, \quad 0(\alpha_i) \geq d] \tag{2-14}$$

where the notation $0(\alpha_i)$ is used to represent the order of the received bit in error. The evaluation of this upper bound can be difficult, depending on the particular channel models, but its close relationship to selection diversity results provides some insight. Note that for selection diversity an error is made if the highest ranked bit is incorrect, which is similar to the above probability. For a more general class of channel measurement decoding algorithms, it has been shown [6] that

$$P_e[\text{block}] < \binom{N}{d} P_e^{\,d}[d\text{th order diversity}] \tag{2-15}$$

where the diversity error probability above is obtained by summing together d weighted decision statistics. While an expression as simple as that given by (2-15) has not been obtained for the decoding algorithm presented in this paper, some preliminary results have been obtained that indicate that this new algorithm is more effective for orthogonal codes than the more general algorithm previously presented.

The actual coding transformation used in Codem I is similar to the (9,4) product code discussed previously. Since 25 tones are phase keyed with 2 bits (four phases) per tone, 50 bits must be supplied to the modulator each frame or keying interval. In order to have errors occurring as independently as possible, two separate codes (one for the in-phase and the other for the quadrature component of a given tone) are used. In particular, two (25, 16) product codes obtained by arranging the information sequences in a 4 X 4 matrix are used to phase key the 25 tones. Since, in general, for a fading channel there is a dependence between adjacent tones, the codeword is scattered across the 25 adjacent tones as illustrated in Fig. 5. This particular transformation has the property that any given row or parity equation is formed from tones that are spaced by at least four harmonics. This scattering of code bits across the frequency band tends to minimize the probability of having more than one error occurring in a given parity equation, which increases the effectiveness of this decoding algorithm.

In addition to using channel measurement information to increase the efficiency of the decoding process, the Codem I system also uses channel measurement information to label blocks of data that have a high probability of containing incorrect data. This feature is quite important for communications applications where incorrect data are considerably more detrimental to the overall system than no data at all.

In the Codem I system a block of decoded data is accepted if the sum of the confidence values of the inverted bits is less than or equal to the variable threshold given by the sum of the confidence values of the K lowest ranked bits. This criterion for acceptance of data can be written as

$$\sum_{i \epsilon S_X} \alpha_i \leqslant \sum_{i \epsilon S_K} \alpha_i \tag{2-16}$$

where S_X is the set of bits that is inverted and S_K is the set of bits of rank less than K.

For the Codem I computer-simulated results given in Section IV a threshold based on the $K = 3$ lowest confidence levels is used. This choice of threshold is somewhat arbitrary. One would increase the value of K for applications where the percentage of data rejection must be decreased.

1	6	11	16	21
22	2	7	12	17
18	23	3	8	13
14	19	24	4	9
10	15	20	25	5

Fig. 5. Basic (25, 16) product code transformation. Numbers indicate the particular tones that form a given parity equation.

III. Description of the Channel Models

Three different channel models are described in this section. All of these models exhibit selective fading, which is characteristic of dispersive channels, but have significant differences that affect the performance of the particular signaling scheme. For this reason, some care is taken to specify these models in sufficient detail so that computer simulations under identical conditions can readily be reproduced.

A. Model 1—Independent Rayleigh Fading Model

This model assumes that adjacent frequency tones are uncorrelated with each individual tone having a Rayleigh amplitude and a uniform phase distribution. Thus, if we transmit a set of N orthogonal tones given by

$$x(t) = \sum_{i=1}^{N} \sqrt{2} \cos \omega_i t \tag{3-1}$$

with

$$\frac{1}{T}\int_0^T (\sqrt{2}\cos\omega_i t)(\sqrt{2}\cos\omega_j t)\,dt = \begin{cases} 1, & i=j \\ 0, & i\neq j \end{cases} \tag{3-2}$$

we receive a signal of the following form:

$$y(t) = \sum_{i=1}^{N} \sqrt{2}\, r_i \cos(\omega_i t + \gamma_i) + n(t). \tag{3-3}$$

The amplitude distribution of each tone r_i is assumed to be Rayleigh with

$$E[r_i r_j] = \begin{cases} S^2, & i=j \\ 0, & \text{otherwise,} \end{cases} \tag{3-4}$$

where S^2 is the average power in each tone. The received phase angles γ_i are independent and uniformly distributed. The additive noise is represented by $n(t)$.

The Rayleigh amplitude and uniform phase distributions are obtained by considering two independent zero mean Gaussian variables x_i and y_i, where the Rayleigh amplitude is given by

$$r_i = \sqrt{x_i^2 + y_i^2} = |x_i + jy_i| \tag{3-5}$$

and the uniform phase is given by

$$\gamma_i = \tan^{-1}(y_i/x_i). \tag{3-6}$$

The variance of each of these Gaussian variables is chosen such that

$$E[r_i^2] = E[x_i^2] + E[y_i^2] = 2E[x_i^2] = S^2 \tag{3-7}$$

to give the correct tone power.

The additive noise components for each tone

$$n_{ci} = \frac{1}{T}\int_0^T \sqrt{2}\, n(t) \cos \omega_i t\, dt \tag{3-8}$$

and

$$n_{si} = \frac{1}{T}\int_0^T \sqrt{2}\, n(t) \sin \omega_i t\, dt \tag{3-9}$$

are independent Gaussian variables where, as previously mentioned, $n(t)$ is assumed to be a white Gaussian noise process with a one-sided noise spectrum given by N_0. Thus, the signal-to-noise ratio per tone can be written as

$$\gamma = \frac{E[r_i^2]}{E[n_{ci}^2] + E[n_{si}^2]} = \frac{S^2}{2\sigma^2} = \frac{S^2 T}{N_0} \tag{3-10}$$

where $\sigma^2 = N_0/2T$ is the variance of n_{ci} and n_{si}.

To simulate four-phase DPSK over this model we generate a set of reference tones that satisfy (3-4)-(3-10) and in complex notation are given by

$$v_i' = r_i' \underline{/\gamma_i'} + n_{ci}' + jn_{si}', \qquad i = 1, 2, \cdots, N. \tag{3-11}$$

These tones are compared to the information tones given by

$$v_i = r_i \underline{/\gamma_i + \theta_i} + n_{ci} + jn_{si}, \tag{3-12}$$

where the information phase θ_i is given by $\pm\pi/4$ or $\pm 3\pi/4$. The reference tones actually correspond to the information tones of the previous frame and θ_i corresponds to the information phase change from frame to frame. Without loss in generality this angle can be fixed at $\pi/4$, which can be viewed as a data stream of all zeroes.

For the slowly fading case, we assume that $r_i' = r_i$ and $\gamma_i' = \gamma_i$, with additive noise components n_{ci}, n_{si}, n_{ci}, and n_{si} all being independent. A raw bit error is made if the noise is such that the DPSK receiver indicates that a 1 rather than a 0 is transmitted, i.e., the projection on the X or Y axis is negative. Equations (3-1)-(3-12) are used to simulate a single frame of data. This process is repeated, i.e., an entirely new set of reference and information tones is generated for a simulation covering many frames of data.

B. Model 2–Correlated Rayleigh Fading Model

For this model the fading between adjacent frequency tones is correlated. Thus, the expected value of $r_i r_j$ $(i \neq j)$ is no longer zero as assumed in (3-4) for the independent fading model. In particular, a Gaussian correlation was chosen between the set of x_i and the set of y_i that are used in (3-5) to obtain the set of fading amplitudes given by the value of r_i.

To obtain the correlation between the set of N values of x_i (or y_i) used to generate the frequency tones, we work with a set of zero mean, unit variance, Gaussian random variables given by

$$\boldsymbol{n} = n_0, n_1, n_2, \cdots, n_{N+k-1} \tag{3-13}$$

and a fixed set of k constants given by

$$\boldsymbol{H} = H_0, H_1, H_2, \cdots, H_k. \tag{3-14}$$

This set of constants can be viewed as the impulse responses of the digital filter that is used to generate the correlated set of x_i. For convenience only, the index on the set of N values of x_i will run over the range from $i = k$ to $i = k + N - 1$. Each x_i is given by the convolution

$$x_i = \sum_{l=0}^{k} H_l n_{i-l}, \qquad k \leqslant i < k + N. \tag{3-15}$$

Thus, the first value of x_i is given by

$$x_k = H_0 n_k + H_1 n_{k-1} + \cdots + H_k n_0 \tag{3-16}$$

and the Nth value of x_i is

$$x_{N+k-1} = H_0 n_{N+k-1} + H_1 n_{N+k-2} + \cdots + H_k n_{N-1}. \tag{3-17}$$

The correlation function between these x_i is given by

$$R(\mu) = E[x_{i+\mu}, x_i] = \sum_m \sum_l H_m H_l E[n_{i+\mu-m}, n_{i-l}], \tag{3-18}$$

which for the unit variance independent noise samples is

$$R(\mu) = \sum_m \sum_l H_m H_l \delta_{m-\mu,l} = \sum_{l=0}^{k-\mu} H_{l+\mu} \cdot H_l. \tag{3-19}$$

To obtain the desired value for $R(\mu)$ we work with an impulse response $\boldsymbol{H} = H_0 \cdots H_l \cdots H_k$ given by

$$H_l = C \exp\left[-2a(l - k/2)^2\right], \qquad 0 \leqslant l \leqslant k \tag{3-20}$$

so that

$$R(\mu) = \sum_{l=0}^{k-\mu} C^2 \exp\left[-2a(l + \mu - k/2)^2\right] \exp\left[-2a(l - k/2)^2\right], \tag{3-21}$$

which can be rewritten as

$$R(\mu) = \exp(-a\mu^2) \sum_{l=0}^{k-\mu} C^2 \exp\left[-4a(l - k/2 + \mu/2)^2\right]$$

$$= \exp(-a\mu^2)\left[\sum_{l=\mu/2}^{k-\mu/2} H_l^2\right]. \tag{3-22}$$

The number of discrete samples in $\boldsymbol{H}$ is chosen such that k is much larger than the values of μ of interest, i.e., much larger than the value of μ at the bandwidth of interest. Under these conditions the summation in (3-22) is approximately constant

so that

$$R(\mu) \cong \exp(-a\mu^2)\left[\sum_{l=0}^{k} H_l^2\right], \tag{3-23}$$

which gives us the desired Gaussian correlation between the set of x_i. Each individual x_i, being a weighted sum of Gaussian variables, is still a Gaussian random variable of zero mean and variance given by

$$R(0) = E[x_i^2] = \sum_{l=0}^{k} H_l^2. \tag{3-24}$$

The variance of each x_i is chosen such that

$$\sum_{l=0}^{k} H_l^2 = S^2/2 \tag{3-25}$$

so that

$$E[r_i^2] = E[x_i^2] + E[y_i^2] = S^2, \tag{3-26}$$

the desired tone power. Note that the set of y_i are generated in exactly the same way as the set of x_i.

With $R(\mu)$ given by

$$R(\mu) = \tfrac{1}{2} S^2 \exp(-a\mu^2) \tag{3-27}$$

the correlation coefficient between the set of x_i (or y_i) is given by

$$\rho = \frac{E[x_{i+\mu}, x_i]}{E[x_i^2]} = \exp(-a\mu^2), \tag{3-28}$$

which can be rewritten as

$$\rho = \exp\left[-\frac{a(\mu f_0)^2}{f_0^2}\right] = \exp\left[-\frac{a(\Delta f)^2}{f_0^2}\right] \tag{3-29}$$

where f_0 represents the frequency separation between adjacent tones and $\mu f_0 = \Delta f$ is the frequency separation between x_i and $x_{i+\mu}$, or equivalently, between r_i and $r_{i+\mu}$.

Letting the correlation bandwidth be defined as the bandwidth such that

$$\rho_{B_C} = \exp(-1/2) = \exp\left[-\frac{a(B_C)^2}{f_0^2}\right] = 0.606 \tag{3-30}$$

enables us to solve for the constant a as

$$a = \tfrac{1}{2}(f_0/B_C)^2 \tag{3-31}$$

so that ρ can be rewritten as

$$\rho = \exp\left[-\tfrac{1}{2}(\mu f_0/B_C)^2\right] = \exp\left[-\tfrac{1}{2}(\Delta f/B_C)^2\right]. \tag{3-32}$$

For this definition B_C is just the standard deviation σ of the Gaussian frequency spectrum assumed. Note that the complex correlation function is just the sum of the correlation functions between the set of x_i and the set of y_i and thus its normalized frequency spectrum is the same as above.

In order to completely specify the impulse response H used to generate the correlated variables, the values of a, k, and C in (3-20) must be specified. The value of a can be found from (3-31). For example, if the correlation bandwidth is 500 Hz ($2B_C$, bandwidth between the exp $(-\frac{1}{2})$ points, is 1000 Hz) and the tone separation is 93.75 Hz, then $a = 1.75 \times 10^{-2}$. The value of k is chosen large enough so that the correlation coefficient given by (3-28) is less than 10^{-2} at $\mu = (k-1)/2$. A value of $k = 35$ is sufficient. Once the constants a and k are chosen, the value of C in (3-20) is chosen by (3-25) to give a desired tone power. A correlation bandwidth of $B_C = 500/n$ Hz can also readily be obtained from the above samples by just reading out every nth sample for the x_i and y_i components of r_i. This is equivalent to increasing the value of a by n^2 as is required for a correlation bandwidth of $500/n$.

C. Model 3—Time-Varying Multipath Model

For this channel we assume that the single-path response to a set of orthogonal tones given by (3-1) is

$$y(t) = \sum_{i=1}^{N} \sqrt{2}\, r(t) \cos(\omega_i t + \gamma(t)) + n(t), \tag{3-33}$$

where $r(t)$ and $\gamma(t)$ are time varying and obtained from a complex Gaussian process whose autocorrelation is Gaussian distributed. Thus the autocorrelation of the x and y components used to generate r and γ is given by (3-27) as in the previous model. However, in this case the correlation function is computed in time rather than in frequency. This correlation function can be written in terms of the fading bandwidth B as

$$R(\tau) = \tfrac{1}{2} S^2 \exp(-2\pi^2 B^2 \tau^2) \tag{3-34}$$

so that its spectrum is given by

$$S(f) = \frac{S^2}{2B\sqrt{2\pi}} \exp\left[-\tfrac{1}{2}(f/B)^2\right]. \tag{3-35}$$

The fading bandwidth above is defined as the standard deviation σ of the fading spectrum, which also corresponds to the point where the correlation coefficient is down to exp $(-1/2) = 0.606$.[2]

To simulate this model (3-13)-(3-28) still apply except now μ is a discrete number of time frame intervals whereas previously μ represented a discrete number of frequency harmonics. The time correlation coefficient can now be written as

$$\rho = \exp(-a\mu^2) = \exp\left[-a(\mu T_f/T_f)^2\right] = \exp\left[-a(\tau/T_f)^2\right], \tag{3-36}$$

where T_f is the time between data frames and μ is number of frames over which this correlation coefficient is computed. As noted previously [see (2-4)] T_f is somewhat longer than the integration time T used in (3-2) because of the guard time assumed for these parallel tone modems. The value of a in (3-36) can be obtained from (3-34) and is given by

$$a = 2\pi^2 (BT_f)^2. \tag{3-37}$$

Thus, for a fading bandwidth of $B = \frac{1}{8}$ Hz and $T_f = \frac{1}{75}$ s, we

[2] The fading bandwidth has also been defined as the point where the correlation coefficient is ½ (half-power) in [1]. The half-power fading bandwidth $B_{HP} = B\sqrt{2 \ln (2)} = 1.18B$ and thus the two definitions are almost equivalent.

obtain a value of $a = 5.5 \times 10^{-5}$. In order for the correlation coefficient to be below 10^{-2} at $\mu = (k - 1)/2$ the digital filter given by (3-14) must have $k = 581$ coefficients. Fading bandwidth of $n/8$ Hz can also be obtained by reading out every nth sample, which has the effect of increasing the value of a by n^2.

A time-varying single-path model does exhibit frequency spreading, which was assumed negligible in models 1 and 2, but does not exhibit selective fading due to multipath. Note that the frequency spectrum is completely flat with all tones having the same amplitude and phase for the single-path model. By including another independent path delayed by τ_0 relative to the first path, a more typical channel model results.

The channel response due to (3-1) is now given by

$$y(t) = \sum_{i=1}^{N} \sqrt{2} r_A(t) \cos(\omega_i t + \gamma_A(t)) + \sum_{i=1}^{N} \sqrt{2} r_B(t) \cos(\omega_i (t - \tau_0) + \gamma_B(t)) + n(t) \quad (3\text{-}38)$$

where $r_A(t)$ and $r_B(t)$ are the fading amplitudes associated with the first and second paths, respectively. The average signal power per tone is still held constant by requiring that

$$S^2 = E[r_A^2] + E[r_B^2]. \quad (3\text{-}39)$$

For a given frame interval the amplitude and phase of each received tone is held fixed by this model and thus is given by

$$v_i = r_A \angle \gamma_A + r_B \angle \gamma_B - \omega_i \tau_0 + n_{ci} + j n_{si} \quad (3\text{-}40)$$

for $i = 1, 2, \cdots, N$. This equation is analogous to (3-11) except now the variation in amplitude and phase across the frequency band are due to $\omega_i \tau_0$ rather than the statistical relationship between r_i and r_j. Since (3-40) will be time varying in discrete frame interval steps, it is no longer necessary to generate an independent reference vector for each data frame as is required for models 1 and 2. In our simulations we will use a two-path model with $\tau_0 = 1$ ms.

A refinement on this channel model can be made by letting the fading parameters vary in discrete steps that are small compared to T_f, the frame interval. This would allow the effects of time variation over a frame interval to be included in (3-40). The cross terms from the adjacent frequency resulting from this loss of orthogonality will contribute in the same manner as the additive noise terms $n_{ci} + j n_{si}$. Thus, one need only include this effect if the simulated additive noise term is so low that it is comparable to the crosstalk introduced by the time variations.

D. Discussion of Channel Models

The independent Rayleigh fading model is attractive from an analysis point of view, but is somewhat unrealistic for a parallel tone signaling scheme where successive tones are closely spaced in frequency. In Fig. 6, a computer-generated frequency spectrum of the amplitude (r_i) of a set of 25 tones is shown for several independent frames. This figure should be compared with Fig. 7, which shows the same plot for model 2 where the two-sided correlation bandwidth ($2B_c$) is 1000 Hz. Both of

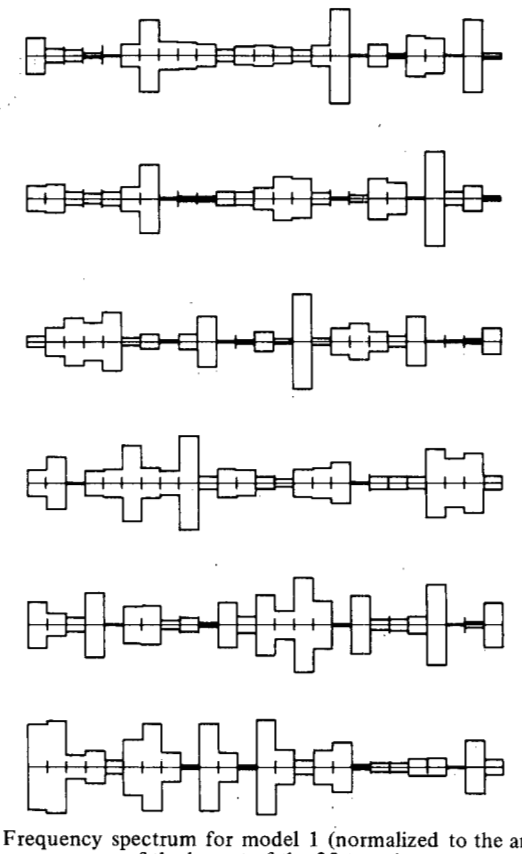

Fig. 6. Frequency spectrum for model 1 (normalized to the amplitude of the largest of the 25 tones).

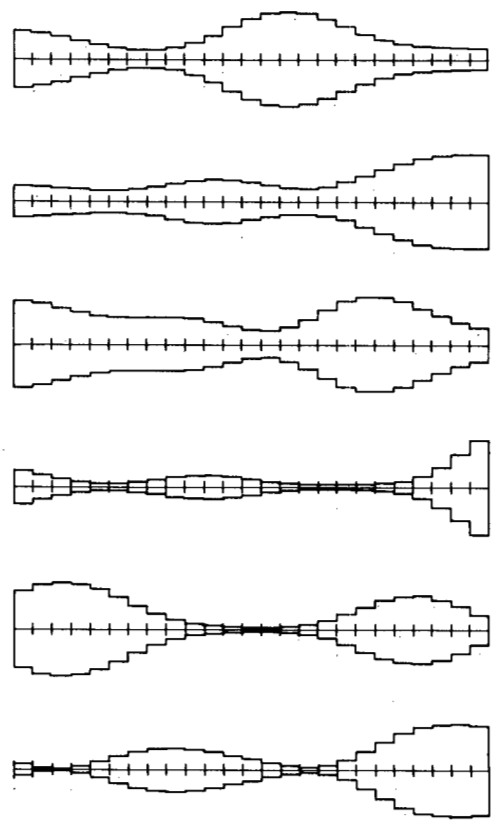

Fig. 7. Frequency spectrum for model 2 with $2B_C = 1000$ Hz (25 tones are spaced at 93.75-Hz intervals).

these models exhibit deep fading well below a factor of 10 in amplitude (20 dB) within the frequency band which, indeed, is a motivation for applying error correction across the frequency band. The correlation introduced in model 2 can yield frequency spectra that have fades that extend over many successive tones. Needless to say, fades of this nature will limit the effectiveness of coding as will be illustrated when the error rate possible on model 2 is compared to the results obtained on model 1.

The frequency spectrum resulting from a two-path (τ_0 = 1 ms) time-varying model is obtained from (3-40) (with the additive noise omitted) and is shown in Fig. 8. Since this model is time varying, the fade rate shown is $2B = \frac{1}{4}$ Hz, successive frames change slowly with time. Every 100th frame is shown, which corresponds to a time interval of $100(T_f)$ = 1.33 s between the adjacent spectra. This model has been compared with the actual HF data [7] and is attractive since it exhibits both selective fading and time variation. A plot of the actual received signal power in a single path as a function of time is shown in Fig. 9. The received power is normalized relative to its average power and is plotted in decibels. A fade rate of $2B = \frac{1}{4}$ Hz was chosen for this plot. This plot illustrates the deep fades that can occur in time and that affect the entire frequency band. This phenomenon does not appear in the frequency spectra shown since they were normalized to the amplitude of the largest tone present. Actual HF frequency spectra previously published [8] compare favorably with the spectra illustrated for models 2 and 3.

A plot of time variation in signal power for models 1 and 2 is fairly uninstructive since every frame, and its corresponding reference, is independently selected and thus the power is different in every successive frame. However, the frequency correlation for model 2 makes the variance of its average power across the band of 25 tones considerably greater than the variance of average power of model 1, which is composed of 25 independently fading tones.

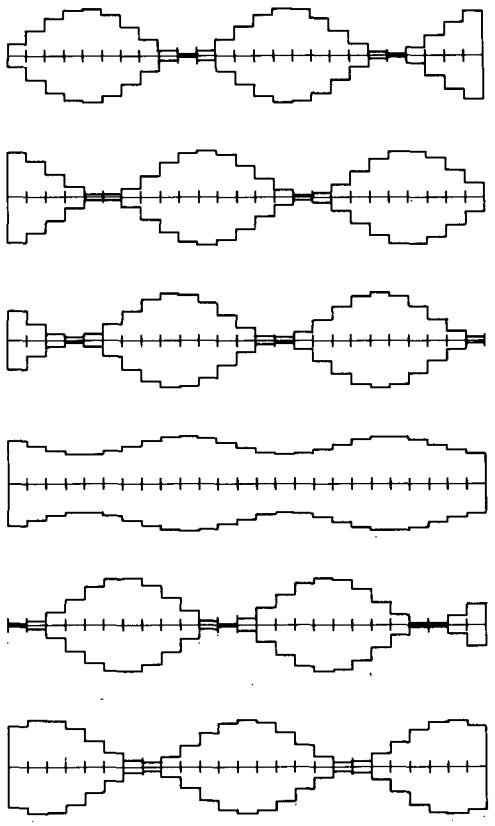

Fig. 8. Frequency spectrum for model 3 with τ_0 = 1 ms and $2B = \frac{1}{4}$ Hz (spectra of 25 tones spaced 93.75 Hz apart are shown with a time interval of 1.33 s between adjacent spectra).

IV. Computer-Simulated and Field-Test Results

In this section computer-simulated results and some field-test data for Codem I will be presented. The emphasis will be on comparing the performance of a conventional 16-tone modem to the 25-tone Codem. Both data terminal sets operate at 2400 bits/s in a single voice band and utilize four-phase DPSK. A summary of the parameters that define each system is given in Table I.

In many cases the performance of modems is shown by a bit error P_e as a function of the signal-to-noise ratio per tone. This parameter, given by (3-10), is useful when we are comparing modems with identical modulation formats since theoretical results are generally plotted as a function of γ. However, in our case the probability of a bit error will be plotted as a function of the received energy per information bit E_b divided by noise per unit hertz N_0. The total received power P_r divided by the data rate R is just the energy per information bit. Thus we can write

$$E_b/N_0 = P_r/RN_0, \tag{4-1}$$

which is relatively easy to obtain experimentally by measuring P_r and N_0.

In order to relate E_b/N_0 to the signal-to-noise per tone used to specify the computer models given in Section III we note that the received power is given by

$$P_r = (16 + 2^2)S^2 \tag{4-2}$$

for a 16-tone modem and

$$P_r = (25 + 2^2)S^2 \tag{4-3}$$

for Codem I. The power per tone is given by S^2 and the factor $4S^2$ is the power in the unkeyed tone used for fixed Doppler correction. The noise power per tone $2\sigma^2$ is given in terms of N_0 as

$$2\sigma^2 = N_0/T = N_0 f_0 \tag{4-4}$$

where T is the integration time that is the reciprocal of f_0 the frequency separation (f_0 = 110 Hz for the 16-tone modem and 93.75 Hz for Codem I). Substituting these results into (4-1) yields

$$\frac{E_b}{N_0} = \frac{20S^2}{R(2\sigma^2/f_0)} = \frac{2200}{2400}\gamma \qquad \text{16-tone modem} \tag{4-5}$$

and

$$\frac{E_b}{N_0} = \left(\frac{29f_0}{R}\right)\left(\frac{S^2}{2\sigma^2}\right) = \frac{2718.75}{2400}\gamma \qquad \text{Codem I.} \tag{4-6}$$

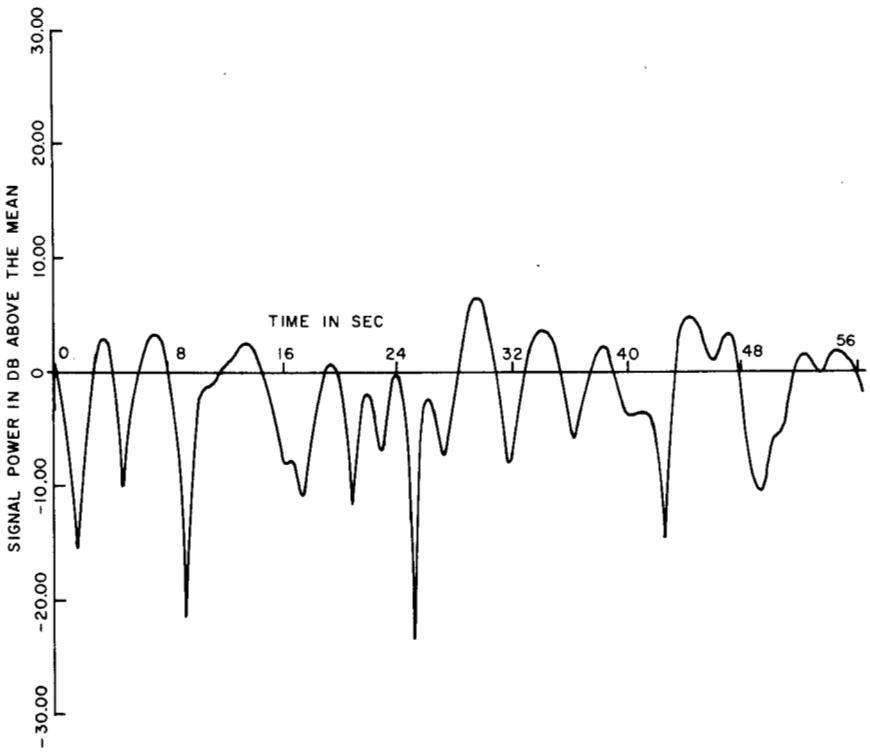

Fig. 9. Single-path time-varying model–fade rate $2B = \frac{1}{4}$ Hz.

TABLE I
PARAMETERS FOR CODEM I AND A 16-TONE MODEM

	Codem I	16-Tone Modem
Data rate R	2400 bits/s (coded data rate = 3750 bits/s)	2400 bits/s
Frame rate T_f	75 frames/s	75 frames/s
Information bits/frame	32 bits/frame	32 bits/frame
Modulation	4Ø DPSK (2 bits/tone)	4Ø DPSK (2 bits/tone)
Coding transformation	50 bits are obtained from two (25, 16) product codes with each of the 25 tones containing one digit from each code	32 bits are used to phase key 16 tones
Tone separation f_0	93.75 Hz	110 Hz
Integration time T	10.67 ms	9.1 ms
Guard time T_g	2.67 ms	4.23 ms
Tone library	468.75: unkeyed Doppler correction tone at twice the amplitude of data tones 656.25–data 1 750.00–data 2 . . . 2906.25–data 25	605: unkeyed Doppler correction tone at twice the amplitude of data tones 935–data 1 1045–data 2 . . . 2585–data 16

An alternative way of obtaining the same factor relating γ and E_b/N_0 is to start with E_b/N_0 and find the necessary factors required to obtain γ. For a 16-tone modem we obtain $\gamma = (E_b/N_0)$ (2 bits/tone) (16/20 loss due to Doppler tone) · (75/110 loss due to guard time) and for Codem we obtain $\gamma = (E_b/N_0)$ (2 bits/tone) (16/29 loss due to Doppler tone and code rate) (75/93.75 loss due to guard time).

Writing these results in terms of decibels we have

$$E_b/N_0 = \gamma - 0.37 \qquad \text{16-tone modem}$$

and

$$E_b/N_0 = \gamma + 0.53 \qquad \text{Codem I} \tag{4-7}$$

and thus the Codem used 0.9 dB less power per tone for constant received power. The error-correcting capabilities of Codem more than compensate for this slight loss in power per tone as will be illustrated by the performance curves to follow. It should be noted that by plotting P_e as a function of E_b/N_0 enables one to compare the modem and Codem at equal re-

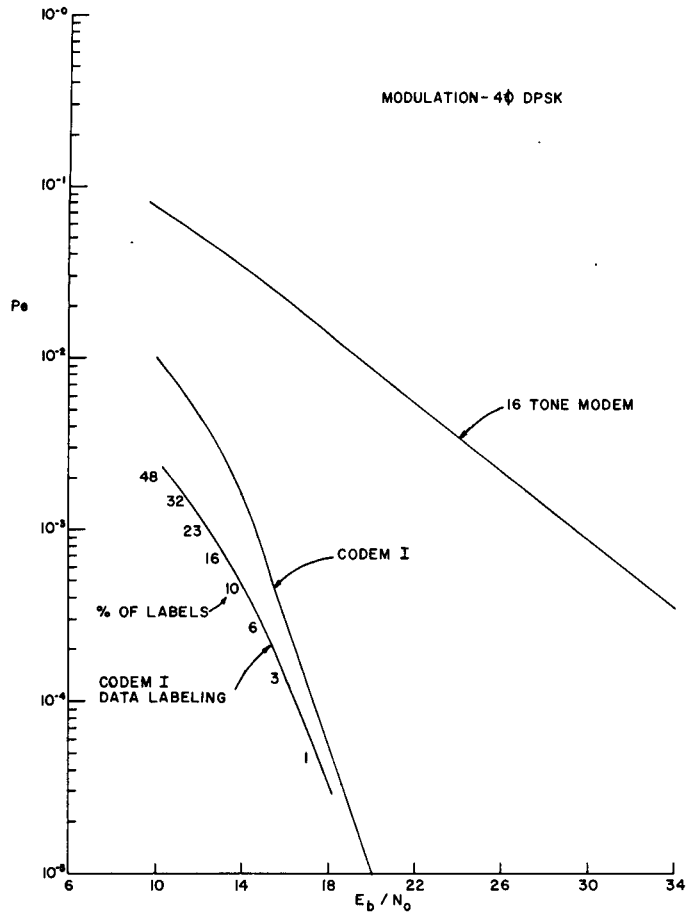

Fig. 10. Computer-simulated performance comparison for the independent Rayleigh fading model.

ceived power and at an equal data rate of 2400 bits/s. Both systems operated within a voice bandwidth channel; however, the 16-tone modem requires about 20 percent less bandwidth than Codem I.

A comparison of Codem I and the 16-tone modem is illustrated in Fig. 10 for model 1—the independent Rayleigh fading model. A key feature of this performance curve is the rate of change of the probability of bit error with E_b/N_0. For an uncoded modem a 10-dB increase in signal power is needed for an order-of-magnitude decrease in the probability of error. For the Codem I the probability of error drops at the rate of 2.5 dB per order of magnitude. The amount of data rejected, based on a threshold set at the sum of the bits with the three lowest confidence values, decreases with increasing signal-to-noise ratios and the corresponding performance improvement also decreases as E_b/N_0 increases. The behavior of Codem I with data rejection on these computer models will differ significantly from the data rejection performance measured during field testing. This is a point that will be discussed further.

Before discussing the more complex channel models, some insight into the expected performance of this channel measurement decoding algorithm can be obtained by deriving a lower bound on its performance. Actually, the bound to be presented is a lower bound on the performance of all possible decoding algorithms.

We start by noting that regardless of the particular decoding scheme a sufficient condition for a block error is the occurrence of a received sequence that is a legitimate codeword and not equal to the transmitted codeword. Since all parity equations check in this case, the optimum receiver must accept the sequence as is and thus errors will be made. For a code of minimum distance d, the number of sequences that are codewords and have exactly d errors is the number of codewords of weight d, which we denote by n_d. By calculating the probability of the occurrence of only these n_d sequences we obtain the following lower bound on a codeword:

$$P_e\,(\text{word}) > n_d\, p^d\, (1-p)^{N-d}, \tag{4-8}$$

which is valid for raw bit errors occurring independently with a probability of p as is the case for channel model 1. Note that for a four-phase modulation scheme the pair of bits on a given tone are a function of the same fading variable and are thus dependent. However, in Codem I, two separate (25, 16) codewords are used to isolate the pair of dependent bits so that within a codeword the raw bit errors occur independently.

For the (25, 16) product code illustrated in Fig. 5 we calculate n_d ($d=4$) by noting that four errors must occur in a rectangular pattern to yield a codeword. There are $\binom{5}{2}$ ways of choosing the columns for this rectangular pattern and $\binom{5}{2}$ ways of choosing the rows. The product of these two numbers yields $n_d = 100$ for this code. In order to convert the lower bound given by (4-8) into a bound on P_e, the probability of a bit error, we note that each codeword of 25 bits will contain four errors so that the bound must be reduced by the factor 4/25. Thus, we obtain

$$P_e > 16p^4\,(1-p)^{21} \tag{4-9}$$

as a lower bound on all decoders.

For four-phase DPSK the value of p for the Rayleigh fading channel is [9]

$$p = \tfrac{1}{2}\,[1 - \gamma/\sqrt{\gamma^2 + 4\gamma + 2}], \tag{4-10}$$

where γ is the signal-to-noise ratio per tone. Evaluating (4-9) for high signal-to-noise ratios yields a probability of error that decreases by a constant time $1/\gamma^4$, or 2.5 dB per order of magnitude. This is the same rate of decrease as was obtained by simulation of the decoding algorithm presented. These results at least indicate that the slope of the performance of this channel measurement decoding algorithm cannot be improved.

A tight upper and lower bound of the performance of a conventional binary decoder will be obtained for a minimum distance 4 code such as the (25, 16) code under consideration. These results will enable us to compare the given algorithm with conventional binary decoders as well as optimum decoders. A conventional decoder can correct all single errors and detect an even number of errors. If the number of raw bit errors in a code block is an even number, the decoder will not add or remove any of these errors. However, if there are an odd number of raw bit errors in the block, the decoder will take action. A single error will be corrected, but an odd number of raw bit errors greater than one will not be corrected. Furthermore, the decoder may add an additional error when correction is attempted in these cases. Thus, an upper bound

on the average number of errors in a block of N digits is given by

$$NP_e \leqslant \sum_{i \text{ even} \geqslant 2} i \Pr [i \text{ raw bit errors}] + \sum_{i \text{ odd} \geqslant 3} (i+1) \Pr [i \text{ raw bit errors}]. \quad (4\text{-}11)$$

Equation (4-11) can be upper bounded further by

$$NP_e \leqslant 2 \Pr [2 \text{ raw bit errors}] + \sum_{\text{all } i \geqslant 3}^{N} (i+1) \Pr [i \text{ raw bit errors}] \quad (4\text{-}12)$$

by replacing i by $i+1$ for all i even $\geqslant 4$.

The probability of having i raw bit errors in a block of N digits is given by

$$\Pr [i \text{ raw bit errors}] = \binom{N}{i} p^i (1-p)^{N-i} \quad (4\text{-}13)$$

for the case when errors occur independent with probability p.

Substituting (4-13) into (4-12) gives

$$NP_e \leqslant 2\binom{N}{2} p^2 \cdot \left[(1-p)^{N-2} + \sum_{i \geqslant 3}^{N} (i+1) \frac{\binom{N}{i} p^i (1-p)^{N-i}}{2\binom{N}{2} p^2} \right],$$

which can be rewritten as

$$NP_e \leqslant 2\binom{N}{2} p^2 \left[(1-p)^{N-2} + \sum_{i \geqslant 3}^{N} \frac{(i+1)}{i(i-1)} \binom{N-2}{i-2} p^{i-2} (1-p)^{N-i} \right]. \quad (4\text{-}14)$$

Since $i \geqslant 3$ we have

$$\frac{i+1}{i(i-1)} < 1 \quad (4\text{-}15)$$

enabling us to upper bound (4-14) by

$$NP_e \leqslant 2\binom{N}{2} p^2 \left[(1-p)^{N-2} + \sum_{j=1}^{N-2} \binom{N-2}{j} p^j (1-p)^{(N-2)-j} \right], \quad (4\text{-}16)$$

where $i-2$ is replaced by j in (4-16). Since the term in brackets is just equal to 1, we now have

$$NP_e \leqslant 2\binom{N}{2} p^2 \quad (4\text{-}17)$$

or

$$P_e \leqslant (N-1) p^2, \quad (4\text{-}18)$$

which is the desired upper bound on P_e.

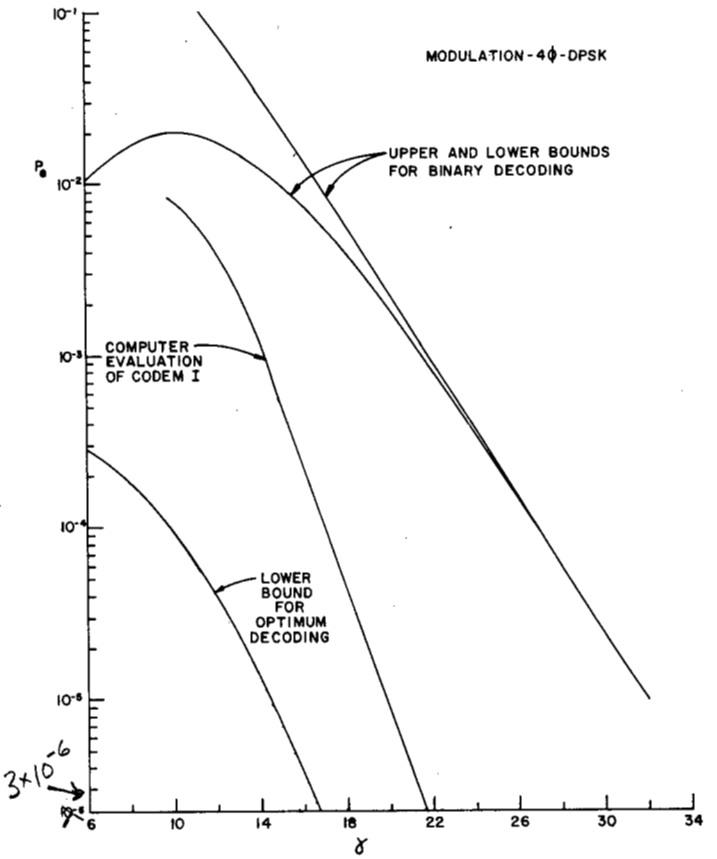

Fig. 11. Comparison of conventional binary and channel measurement decoding for the independent Rayleigh fading model.

To obtain a lower bound on P_e we note that the average number of errors in a block after decoding must satisfy

$$NP_e \geqslant 2 \Pr [2 \text{ raw bit errors}] \quad (4\text{-}19)$$

since we are neglecting the cases when more than two raw bit errors occur.

Substituting (4-13) into (4-19) gives the desired lower bound

$$P_e \geqslant (N-1) p^2 (1-p)^{N-2}. \quad (4\text{-}20)$$

For the (25, 16) product code the upper and lower bounds are thus given by

$$(24) p^2 (1-p)^{23} \leqslant P_e \leqslant (24) p^2. \quad (4\text{-}21)$$

Substituting (4-10) into these bounds shows that for conventional binary decoding P_e decreases with SNR as a constant time $1/\gamma^2$, or 5 dB per order of magnitude.

In Fig. 11 we compare the bounds given by (4-21), the lower bound given by (4-9), and the computer-simulated results obtained on Fig. 10. In this case we have plotted the probability of a bit error (after decoding) as a function of γ, rather than E_b/N_0, since we are only comparing various decoding methods for the Codem I signaling format.

In interpreting the results presented on this graph the 5-dB difference between the lower bound on the computer simulation should not be taken to mean that the given decoding algorithm is 5 dB away from the optimum performance. Remember that the lower bound is based on the occurrence

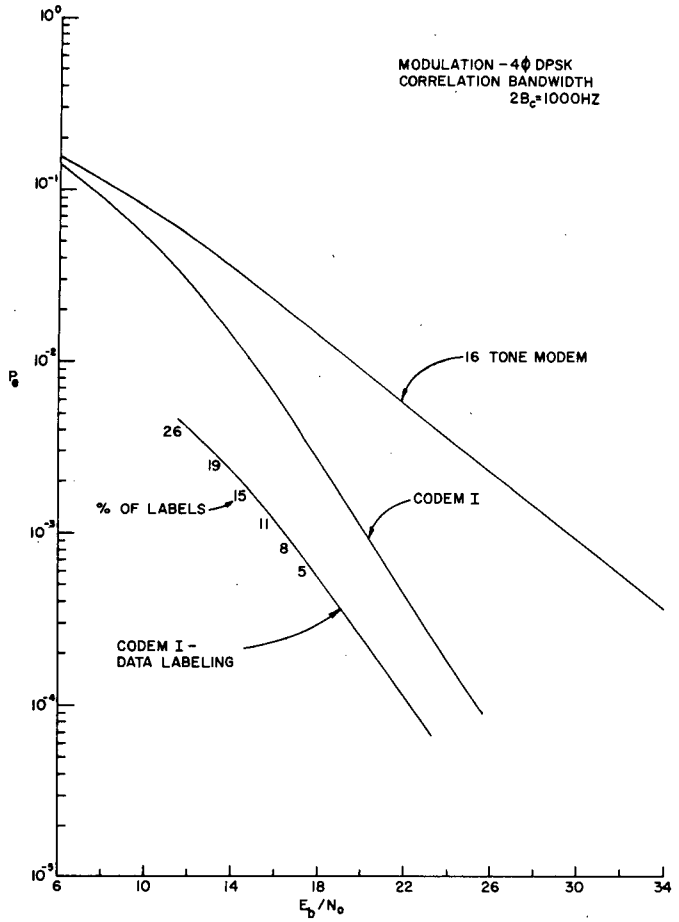

Fig. 12. Computer-simulated performance comparison for the correlated Rayleigh fading model.

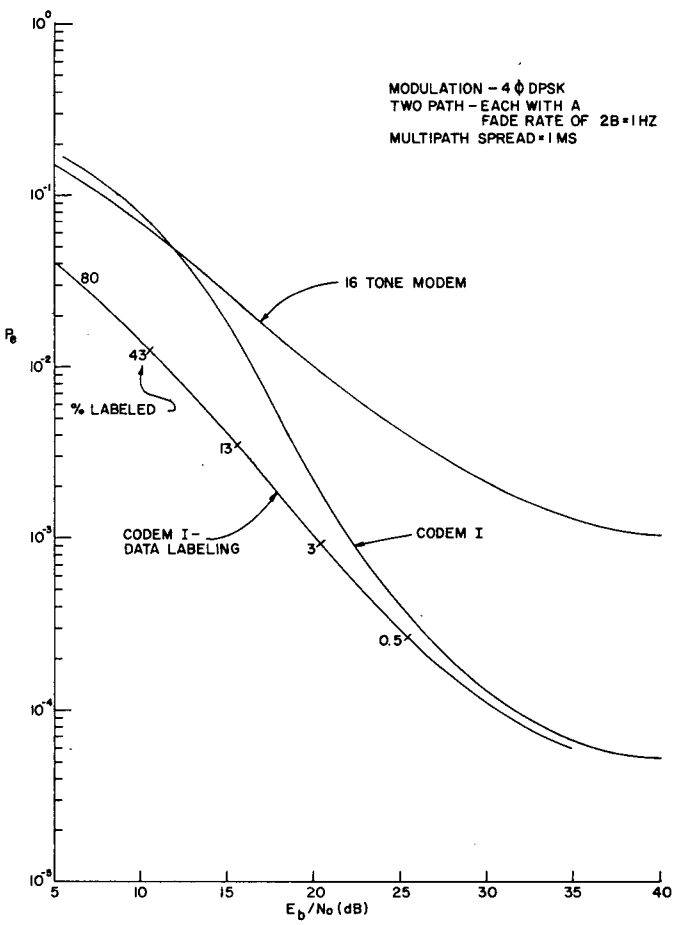

Fig. 13. Computer-simulated performance comparison for the time-varying two-path model.

of a received sequence that is exactly a codeword. This probability yields a fairly loose lower bound even on the optimum channel measurement decoder.

The results obtained for model 2, with correlated bandwidth $2B_c$ = 1000 Hz, are shown in Fig. 12. While the correlation introduced between adjacent tones does not affect the performance of the 16-tone modem, this correlation has a significant effect on the performance of Codem I. A slope that is slightly greater than 5 dB is needed to reduce P_e by an order of magnitude. This rate of change approaches the performance obtained for the independent Rayleigh fading models as the correlation bandwidth is decreased below 1000 Hz. On this model flat fades are more prevalent than on model 1. This phenomenon makes the data-labeling mode more effective since these tones can readily be detected by the data-labeling criteria.

Fig. 13 shows the performance comparison on model 3, simulated with two independently fading paths spread in time by 1 ms and having a fading bandwidth of $2B$ = 1 Hz. This relatively high fading bandwidth was chosen to illustrate the irreducible error resulting from the time variations present in this channel model.[3] Note that even for no additive noise the performance of the 16-tone modem levels off at about 10^{-3} and the performance of Codem I levels off at about 5×10^{-5}. This factor of 20 difference in irreducible errors will increase as the fade rates decrease since the leveling-off effect will start to occur at a higher signal-to-noise ratio than the 30 dB shown on Fig. 13. Note that Codem I has a slope of approximately 5 dB while the 16-tone modem still has a slope of about 10 dB and thus, as the signal-to-noise increases, the differences in performance between these two systems increase.

A field test was conducted to compare the performance of a brassboard model of Codem I with a 16-tone modem during the period of September 21-25, 1971, between Fort Huachuca, Ariz., and Sugar Grove, W. Va. The transmission radio was a TSC-38 located in Fort Huachuca and the receiving radio located in Sugar Grove was an FRR-60.

The radios used had up to four sidebands available and thus data from Codem I and the conventional modem were obtained simultaneously with both systems operating under equal transmission power (approximately 4 kW). During daylight conditions a carrier frequency of about 16 MHz was used with the carrier frequency dropped to about 10 MHz during the night.

The results of the test show the average probability of an error as a function of the percentage of data used to compute the average. The 100 percent point includes all the data collected over a given period, while a 75 percent point deletes the poorest 25 percent of the data. In this way, the error probabilities as a function of the ionospheric conditions can be obtained. It should be pointed out that Codem I was kept on the air until the decoded error rate approached 10^{-2} before changing carrier frequencies. This results in a less favorable error performance at the 100 percent point than would be the case

if frequency changes were made sooner. The conventional modem was unable to operate during the severe conditions (sunset and sunrise) before a frequency change and thus there are no data at the 100 percent point for the 16-tone modem.

Fig. 14 is a typical performance curve based on 86.6×10^6 transmitted bits, which illustrates that over an order-of-magnitude improvement in error performance can be obtained by Codem I when compared to a 16-tone modem. The error rate of Codem I before decoding was also measured and included on Fig. 14. If we compare the improvement due to coding at, for example, the 90 percent point, the error rate before decoding is 10^{-3} and 3×10^{-5} after decoding. These conditions can be justified by models 2 and 3 if the appropriate SNR and fading parameters are assumed; however, the parameters assumed would undoubtedly be incorrect. Note that an additional improvement on the decoded data of two orders of magnitude is obtained by data rejection that is considerably greater than predicted by any of the three channel models. The channel models include only additive Gaussian noise and not atmospheric noise, which is believed to be the cause of this discrepancy. Wide-band impulse-type noise due to atmospherics introduce extremely high raw bit error rates that cannot be corrected by the code but can be rejected by the labeling criteria. Actually, this phenomenon was observed in real time during the field test by test equipment that was capable of measuring the number of raw bit errors within each received code block.

The improvement offered by Codem I for application where 2 percent of the transmitted data can be rejected is at least three orders of magnitude. If model 3 is used to match the performance of Codem with data labeling, the fade rate assumed must be considerably lower than the 1-Hz number used to obtain Fig. 13. Similarly, if model 2 is used, a correlation bandwidth of less than 1000 Hz would be necessary to experience this performance improvement. For the independent Rayleigh fading model an improvement offered by Codem I at a raw error rate (obtained by shifting the curve for the 16-tone modem 0.9 dB to the right) of 10^{-3} is considerably greater than measured, which indicates some correlation between successive tones is necessary to model existing conditions.

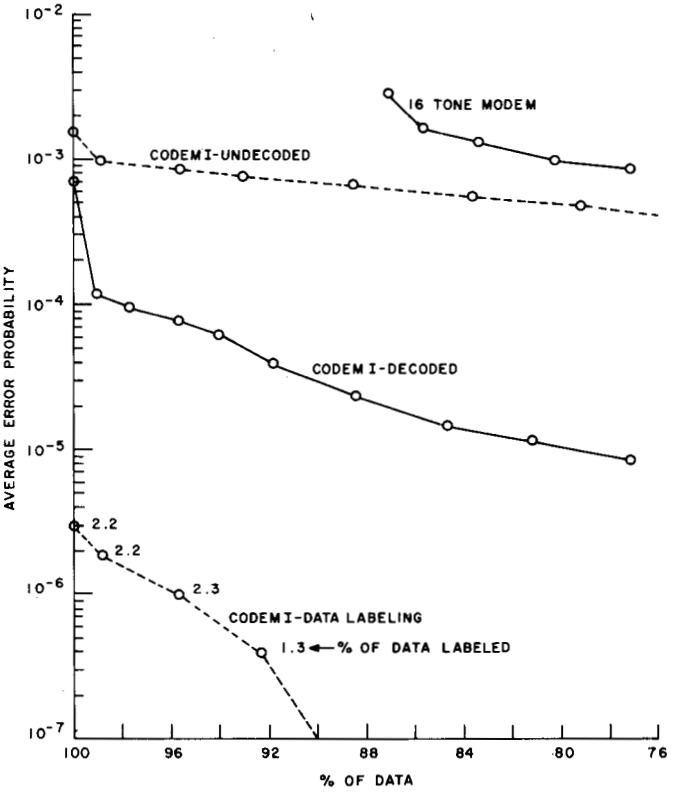

Fig. 14. Field-test results comparing Codem I and a 16-tone modem.

V. Discussion

An approach for obtaining reliable communication over a dispersive channel was presented. The computer simulation results indicate that error-correcting coding combined with channel measurement decoding can offer considerably more than an order-of-magnitude improvement in error performance, which can be traded off for savings in transmitter power exceeding 10 dB. The actual improvement obtained is, however, a strong function of the channel model and the particular fading parameters assumed. In addition to choosing the correct fading parameters, the field test results indicated the importance of including impulse-type noise in addition to the commonly assumed additive Gaussian noise. The use of channel measurement information for rejecting data blocks that are apt to be decoded incorrectly was demonstrated by the field-test results to be particularly effective in the presence of impulse noise.

The comparisons made in this paper between the 25-tone modem were restricted to signaling within a bandwidth of approximately 2.4 kHz and at a data rate of 2400 bits/s. This comparison is quite instructive since both systems are operating at an equal data rate and at the same transmitted power. However, for many HF applications more than one sideband is available for communication. This allows for frequency diversity combining for obtaining an improvement in data reliability. It also, in the case of Codem, allows one to spread the (25, 16) code over more than one sideband, which decreases the dependency between data bits and thus the performance obtained becomes closer to that predicted by model 1—the independent Rayleigh fading model. As a point of interest, Codem I has a mode of operation where two sidebands are used to obtain a data rate of 4800 bits/s. Computer simulation and field-test results demonstrated that the Codem I at 4800 bits/s can outperform a conventional 16-tone modem operating in two sidebands at 2400 bits/s in a dual-frequency diversity mode. This is an example where a coded system is operated over the same channel as the uncoded system but its data rate is twice as great as that for the uncoded system. In the more conventional HF applications of coding [2] the reverse is true, since the coded system operating at 1200 bits/s is compared to the uncoded system operating at 2400 bits/s.

The coding and modulation scheme presented has the property that the data rate is maintained and no additional data delay, beyond one data frame ($\frac{1}{75}$ s), is introduced. The effectiveness of the signaling scheme also increases significantly for applications where data rejection in the order of a few percent is acceptable. However, there are applications where a

continuous flow of unrejected data is required and the initial delay is irrelevant. For applications of this nature the Codem concept can be modified by coding over many frames in such a manner that data that ordinarily would be rejected is completely recovered at a later time. The overall data rate of 2400 bits/s is still maintained by utilizing the data-labeling signal to trap the unreliable code blocks in conjunction with a higher (>16/25) rate code to recover these code blocks. It is believed that a time-domain coding scheme of this nature, combined with the frequency-domain coding scheme already presented, will offer a robust signaling scheme that will be effective over a wide range of channel conditions. This time-domain coding scheme, which will be described in a later article, has recently been implemented but its expected performance improvement in the presence of atmospheric noise has not been demonstrated since this feature was not incorporated into Codem I during the previous field tests.

Acknowledgment

Several people who have had significant influence on the results presented in this paper should be mentioned at this point. R. C. Harper and J. S. Zaborowski, Jr., of General Atronics Corporation have made contributions in the channel-modeling area and are responsible for the computer simulations presented. The actual implementation of the field-tested model of Codem I results largely from the efforts of A. M. Joffe and R. W. Spencer of General Atronics Corporation. F. J. Lueking, E. J. Fabeny, W. E. Gibbons, and W. J. Schoppe of the Department of the Navy provided encouragement and direction in bringing these concepts from the paper to the hardware stage.

References

[1] P. A. Bello and B. D. Nelin, "The influence of the fading spectrum on the binary error probabilities of incoherent and differentially coherent matched filter receivers," *IRE Trans. Commun. Syst.*, vol. CS-10, pp. 160–168, June 1962.
[2] K. Brayer, "Error correction code performance on HF, troposcatter, and satellite channels," *IEEE Trans. Commun. Technol.*, vol. COM-19, pp. 781–789, Oct. 1971.
[3] W. C. Lindsey, "Error probabilities for Rician fading multichannel reception of binary and N-ary signals," *IEEE Trans. Inform. Theory*, vol. IT-10, pp. 339–350, Oct. 1964.
[4] J. C. Massey, *Threshold Decoding*. Cambridge, Mass.: M.I.T. Press, 1963.
[5] R. G. Gallager, *Information Theory and Reliability Communications*. New York: Wiley, 1968.
[6] D. Chase, "A class of algorithms for decoding block codes with channel measurement information," *IEEE Trans. Inform. Theory*, vol. IT-18, pp. 170–182, Jan. 1972.
[7] C. C. Watterson, J. R. Juroshek, and W. D. Bensema, "Experimental confirmation of an HF channel model," *IEEE Trans. Commun. Technol.*, vol. COM-18, pp. 792–803, Dec. 1970.
[8] A. L. Kirsch, P. R. Gray, and D. W. Hanna, Jr., "Field-test results of the AN/GSC-10 (KATHRYN) digital data terminal," *IEEE Trans. Commun. Technol.*, vol. COM-17, pp. 118–128, Apr. 1969.
[9] J. G. Proakis, "Probabilities of error for adaptive reception of M-phase signals," *IEEE Trans. Commun. Technol.*, vol. COM-16, pp. 71–81, Feb. 1968.

David Chase (S'67–M'68) was born in New York, N.Y., on September 16, 1939. He received the B.E.E. degree (magna cum laude) from the City College of New York, New York, in 1962 and the S.M. and Ph.D. degrees from the Massachusetts Institute of Technology, Cambridge, in 1964 and 1967, respectively.

He joined CNR, Inc., Newton, Mass., as Executive Vice President in August 1972. In this position he actively participates in the detailed solution of technical problems concerned with the development of efficient communication and navigation systems. Techniques for optimizing systems by integrating the signal design with the channel and source coding formats are of particular interest to him. During the summer of 1960, he worked in the field of digital communications at the Radio Corporation of America, New York, N.Y.; during the summer of 1961, at the Bell Telephone Laboratories, New York, N.Y.; and, again, at RCA during 1962. The summer of 1964 was spent at the Grumman Aircraft Engineering Corporation, Bethpage, N.Y., where he performed radar system analysis. From 1967 to 1972 he was employed by General Atronics Corporation, a subsidiary of The Magnavox Company, Philadelphia, Pa., as a Staff Engineer and finally as Manager of the Communications Research Department. During this period he also served as a Lecturer for the Graduate School of the Pennsylvania State University, King of Prussia.

Dr. Chase is a member of Eta Kappa Nu, Tau Beta Pi, and Sigma Xi.